Characterization of the Porosity in SBA-15 Silicas by Hyperpolarized ^{129}Xe NMR

A. Nossov,[†] E. Haddad,[†] F. Guenneau,[†] A. Galarneau,[‡] F. Di Renzo,[‡] F. Fajula,[‡] and A. Gédéon*,[†]

Laboratoire des Systèmes Interfaciaux à l'Echelle Nanométrique (SIEN), Université P. et M. Curie, 4 place Jussieu, 75252 Paris Cedex 05 France, and Laboratoire de Matériaux Catalytiques et Catalyse en Chimie Organique, Ecole Nationale Supérieure de Chimie de Montpellier, 8 rue de l'Ecole Normale, 34296 Montpellier Cedex 05 France

Received: July 28, 2003; In Final Form: September 9, 2003

SBA-15 samples prepared at several different temperatures are characterized by hyperpolarized ^{129}Xe NMR spectroscopy. The slope of the chemical shift dependence on pressure allows an evaluation of the xenon−xenon interactions and the size of the micropores at the surface of the SBA-15 mesopores. Samples prepared at 60 °C present micropores larger than 8 Å. Micropore size gradually decreases with the temperature of synthesis, although some surface roughness can be detected even on samples prepared at 130 °C. The decrease of the micropore size with the temperature of synthesis corresponds to a stronger interaction of the adsorbed xenon with the surface. This result is supported by a change of adsorption mechanism as well as by the adsorption enthalpies evaluated from the variation of the ^{129}Xe chemical shift with temperature.

Introduction

SBA-15 mesoporous silicas feature a well-defined hexagonal structure, large surface area, and high hydrothermal stability, which give them high potential for a variety of technological applications. The structural and adsorptive properties of these materials have recently been the subject of extensive studies.[1−5] Despite the ordered hexagonal array of their structural channels, the presence of microporosity and/or disordered openings between channels represents a challenge for every technique of pore size characterization.[6,7] During the past two decades ^{129}Xe NMR has been widely used for the characterization of nanometer-scale void spaces in solids, such as zeolites and clathrates.[8,9] Recently it has been applied for studies of mesoporous silicas[10] and silica glasses.[11] Hyperpolarized (HP) xenon produced by optical pumping methods[12] can attain spin polarizations 10^4 times larger than thermal ones and greatly facilitate the applications of xenon for the characterization of porous materials. In this paper we report the results of HP ^{129}Xe NMR studies of the porosity of SBA-15 silicas prepared at different synthesis temperatures.

Experimental Section

A. Materials. SBA-15 samples have been prepared by using a $(EO)_{20}(PO)_{70}(EO)_{20}$ triblock copolymer and tetraethyl orthosilicate. A precursor mesophase has been formed at 35 °C, and the syntheses have been continued at 60, 100, or 130 °C. In this paper, the three samples used will be identified by their temperature of synthesis in degrees centigrade. All samples have been calcined at 550 °C in air flow and characterized by X-ray diffraction (XRD) and N_2 adsorption at 77 K. N_2 adsorption−desorption isotherms at 77 K for the three samples are reported in Figure 1, and characterization data are reported in Table 1. Cell parameters were determined from XRD, and textural data were characterized by N_2 adsorption at 77 K. The synthesis and characterization of the SBA-15 materials have been described in detail elsewhere.[6]

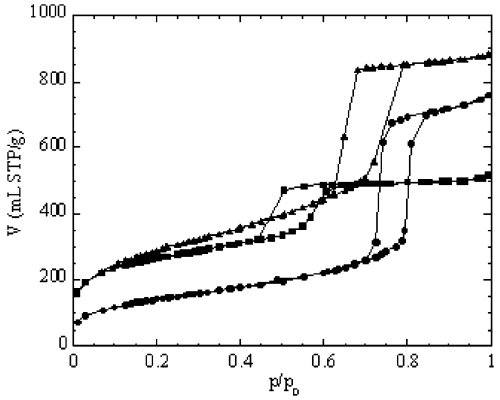

Figure 1. N_2 adsorption−desorption isotherms at 77 K for SBA-15 samples prepared at (▲) 60, (■) 110, and (●) 130 °C.

TABLE 1: Properties of SBA-15 Samples Synthesized at Different Temperature Levels

$T_{synthesis}$ (°C)	a_{hex} (Å)	V_p (mL/g)	D_{BdB} (Å)	S_{BET} (m^2/g)	C_{BET}
60	93	0.75	48	937	−170
110	100	1.32	74	1042	183
130	112	1.11	96	512	121

B. NMR Spectroscopy. Prior to the NMR measurements samples were compressed at 40 MPa, placed in an NMR tube with two Yang valves, and treated at 400 °C overnight. ^{129}Xe NMR spectra were collected on a Bruker AMX 300 spectrometer operating at 83.03 MHz. Hyperpolarized (HP) xenon was produced in the optical pumping cell in the fringe field of the spectrometer magnet. The Xe−He mixtures containing 8−1000 Torr of Xe polarized to ca. 1% at total presssure of 1000 Torr were delivered at 70 cm^3/min flow rate to the samples via plastic tubing. 64−256 FIDs were accumulated with 10 μs (π/2) pulses and 5 s delays.

* Corresponding author. E-mail: ag@ccr.jussieu.fr.
† Université P. et M. Curie.
‡ Ecole Nationale Supérieure de Chimie de Montpellier.

10.1021/jp036195p CCC: $25.00
Published on Web 10/22/2003

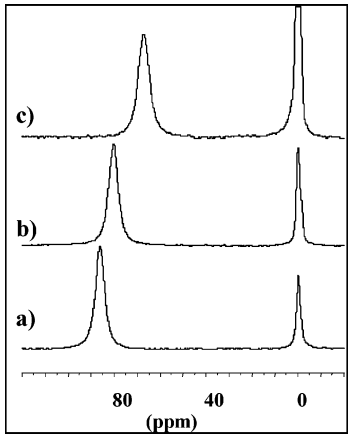

Figure 2. ^{129}Xe NMR spectra of optically polarized xenon at partial Xe pressure of 8 Torr in SBA-15 silicas synthesized at (a) 60, (b) 110, and (c) 130 °C.

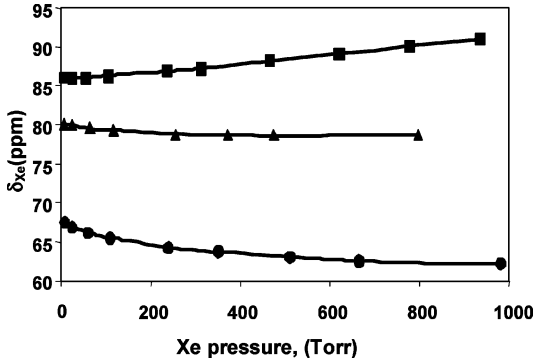

Figure 3. Ambient-temperature ^{129}Xe NMR chemical shift of the resonance line of xenon adsorbed on SBA-15 silicas as a function of pressure. SBA-15 synthesized at (■) 60, (▲) 110, and (●) 130 °C.

Results and Discussion

A. Variable-Pressure Experients. Figure 2 shows the ^{129}Xe NMR spectra of xenon adsorbed on SBA-15 synthesized at different temperature levels. The spectra exhibit the line at 0 ppm from xenon gas in the voids between the particles of the solid and a line shifted to lower field due to xenon adsorbed in the pores. The chemical shift of the line from adsorbed xenon changes from 86.3 to 66.9 ppm with the increase of the synthesis temperature from 60 to 130 °C. The chemical shift of xenon in mesoporous materials depends on the pore size, with the smaller value of the chemical shift corresponding to the bigger pore diameter.[8−10] These changes are in good qualitative agreement with the nitrogen adsorption and XRD data, showing the increase of the pore diameters from 5.0 to 9.5 nm.

Pressure-dependent ^{129}Xe chemical shifts of the studied samples are shown in Figure 3. The rise of the xenon partial pressure from 8 to 1000 Torr for the sample synthesized at 130 °C leads to a decrease of the chemical shift of xenon from 66.9 to 62.2 ppm. The 110 °C sample exhibits a somewhat smaller decrease (from 80.1 to 78.7 ppm) at increasing pressure, whereas for the 60 °C sample an increase of the xenon shift (from 86.1 to 91.0 ppm) is observed when pressure increases.

To understand the observed trends, it is useful to consider the simple model, describing the chemical shift of xenon adsorbed on the mesoporous solid. Under conditions of fast exchange between adsorbed Xe and xenon gas inside the mesopore, the observed chemical shift can be expressed as[10]

$$\delta = p_a\delta_a + p_g\delta_g \quad (1)$$

where $p_a = n_a/(n_g + n_a)$ and $p_g = n_g/(n_g + n_a)$ are the probabilities to find a xenon atom in the adsorbed state and in the gas phase, respectively, and δ_a and δ_g are the chemical shifts of xenon in these phases. If it is assumed that several samples share the same strength of the adsorption sites, viz. the same δ_a, a correlation can be established between the evolution of the chemical shift and the pore size. Consider xenon gas, confined in a long cylindrical mesopore of diameter D. In the case of Henry adsorption,[13] in which the number of adsorbed atoms varies directly with the equilibrium gas pressure, we have

$$n_a = KPS_m \quad (2)$$

where K is Henry's constant and S_m is the surface area of the mesopore. The number of atoms in the gas phase is

$$n_g = PV_m/RT \quad (3)$$

where V_m stands for the volume of the mesopore. Taking $\delta_g = 0$, from eqs 1−3 we have

$$\delta = p_a\delta_a = \delta_a[n_a/(n_g + n_a)] = \delta_a/(1 + n_g/n_a) = \delta_a/(1 + V_m/S_mTKR) \quad (4)$$

Note that δ is independent of Xe pressure, but does depend on the surface-to-volume ratio, which, in principle, is a function of the mean pore diameter. For cylindrical pores ($D = 4V_m/S_m$), eq 4 can be written as

$$\delta = \delta_a/(1 + D/4KRT) \quad (5)$$

Therefore, the chemical shift of xenon adsorbed on a mesoporous solid by Henry-type adsorption should not depend on the Xe pressure. In the case of Langmuir adsorption,[14] with the possibility of a saturation by a single layer of xenon at the surface, the number of adsorbed atoms, n_a, at pressure P is given by

$$n_a = n_0KP/(1 + KP) \quad (6)$$

where n_0 is the number of adsorbed atoms at infinite pressure (i.e., when all sites are filled) and K is the adsorption coefficient. The observed chemical shift of xenon would then depend on the pressure: an increase of the pressure would lead to a decrease of the observed chemical shift. Langmuir adsorption can be expected at a higher coverage, corresponding to a stronger retention of xenon on the adsorption sites. Indeed, the independence of the chemical shift of xenon on pressure was observed for amorphous silicas[10] and MCM-41.[15]

In the case of SBA-15 samples, the pressure dependencies reported in Figure 3 can be explained by the presence of a small number of strong adsorption sites, such as micropore openings on the inner surface of the mesopores. The length of such micropores cannot exceed the wall thickness, and is probably significantly shorter and near 1 nm.[7] In any case, the micropore length is much shorter than the displacement x of the xenon atom due to diffusion, which can be estimated by $x = T_1\sqrt{D}$: taking as a lower limit the value of diffusion coefficient in zeolites $D \sim 10^{-9}$ and a measurement time $T_1^{eff} \sim 1$ s under flow conditions, x is at least 30 μm. Therefore, xenon atoms adsorbed in the micropores are in fast exchange with xenon in mesopores, and their presence can be detected by a variation of the chemical shift of xenon with pressure. The sign of this deviation will depend on the length of micropores. If they are long enough to adsorb several atoms of xenon and large enough to ensure the xenon−xenon interactions, the deviation will be

positive, resembling the typical pressure dependence observed for zeolites. Shallower micropores, in which only isolated atoms of xenon are adsorbed, will give a negative sign of the deviation. The two-site-exchange model proposed in ref 16 can be extended to a three-site model for which the observed chemical shift can be given by

$$\delta = p^{(1)}{}_a\delta^{(1)}{}_a + p^{(2)}{}_a\delta^{(2)}{}_a + p_g\delta_g \quad (7)$$

where $p^{(i)}{}_a = n^{(i)}{}_a/(n_g + \sum n^{(i)}{}_a)$ and $p_g = n_g/(n_g + \sum n^{(i)}{}_a)$ are the probabilities of finding a xenon atom in the adsorbed state at the site (i) ($i = 1, 2$) and in the gas phase, respectively, and $\delta^{(1)}{}_a$ and $\delta^{(2)}{}_a$ are the chemical shifts of xenon atoms adsorbed at two sites with different adsorption constants K_1 and K_2. If $K_1 \gg K_2$, for the stronger adsorption site the Langmuir regime is observed. If the number of sites with large adsorption constant is small enough, the overall dependence of adsorption on pressure in volumetric experiments will not substantially vary from linear.

Using the expressions of adsorbed xenon atoms for Henry (eq 2) and Langmuir (eq 6) adsorption types (sites 1 and 2, respectively), and the number of atoms in the gas phase (eq 3), simple transformations of eq 7 give the following expression for the observed chemical shift:

$$\delta = (A + BP)/(C + DP) \quad (8)$$

where A, B, C, and D are constants dependent on $\delta^{(1)}{}_a$ and $\delta^{(2)}{}_a$, K_1, K_2, and V_m, and P is the xenon pressure. The curve of the pressure dependence for the sample at 130 °C can be fitted using eq 8, but the set of constants obtained is not unique. The pressure dependence of the chemical shift for the three samples (Figure 3) suggests that in the sample formed at 60 °C micropores of zeolitic type are present, large enough to give rise to xenon−xenon interactions inside the micropores, whereas in the sample formed at 130 °C very small micropores are present, able to receive only one xenon atom at a time. In the case of the 110 °C sample the increase of the chemical shift due to xenon−xenon interactions and its decrease because of the presence of shallow micropores counterbalance each other, resulting in a chemical shift practically independent of pressure. This trend provides a new insight into the synthesis of SBA-15, especially the process by which the micropores of the precursor mesophase formed at 35 °C progressively disappear during the second part of the synthesis, carried out at higher temperature.

The C_{BET} energetic parameter of the BET equation for N_2 adsorption has been used to show how the micropore volume of SBA-15 decreases when the synthesis temperature increases. A detailed BET analysis has been carried out on a series of solids including our samples.[6] It has been shown that the C_{BET} parameter (Table 1) passes from negative values to very high and gradually decreasing values as far as the micropore volume decreases. It can be observed that the C_{BET} parameter for the sample prepared at 130 °C is still much higher than the values, usually lower than 100, observed for silica calcined at 550 °C.[6] This shows that some preferred adsorption sites are present in this sample that can be assimilated as very small micropores. Nitrogen adsorption provided no information on the size of the micropores.[6] The *t*-plot of argon adsorption at 77 K suggested the micropores were no larger than 6 Å for a sample synthesized at 60 °C.[7] The slope of the chemical shift vs pressure relation for ^{129}Xe provides further information on the micropore size. The increase of the chemical shift vs pressure indicates that each micropore is large enough to accommodate more than one Xe atom. This suggests that the micropores in the sample

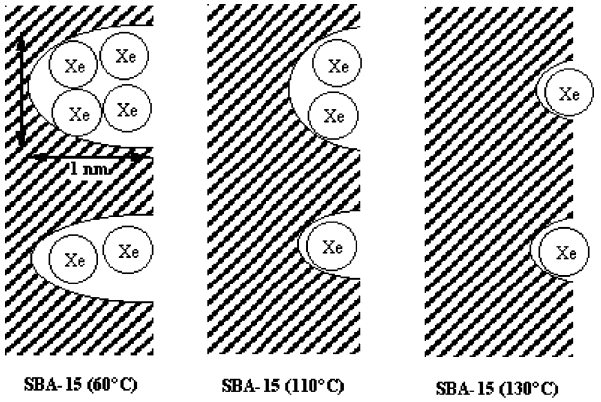

Figure 4. Schematic representation of evolution of microporosity of SBA-15 with synthesis temperature.

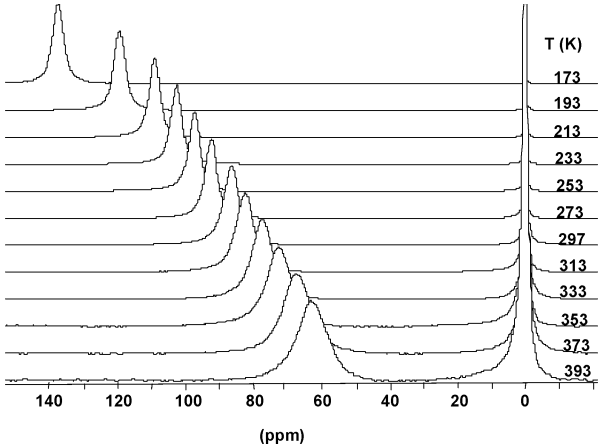

Figure 5. Temperature-dependent ^{129}Xe NMR spectra of optically polarized xenon at partial Xe pressure of 8 Torr in SBA-15 synthesized at 130 °C.

synthesized at 60 °C are larger than twice the kinetic diameter of xenon ($d_{Xe} = 3.96$ Å) along at least one direction. Such a size would be in fair agreement with the genesis of the micropores, formed by the polymerization of silica around loops of the poly(oxyethylene) chains, normally protruding up to 9 Å from the surface of a micelle of nonionic surfactant.[17] For the sample synthesized at 130 °C, the dependence of ^{129}Xe chemical shift on pressure suggests the micropores to be smaller than twice the kinetic diameter of xenon both in depth and in width. Such shallow micropores would be at the borderline with surface roughness, usually defined as cavities with a depth no larger than their width, and could hardly be detected by N_2 and Ar adsorption.[6,7]

The evolution of the micropore size is qualitatively depicted in Figure 4. The shrinking of the micropores with the temperature of the final phase of the synthesis suggests a mechanism akin to sintering for the gradual shrinking of the micropores of the precursor mesophase. The main conclusion suggested by the evolution with pressure of the chemical shift of ^{129}Xe is that SBA-15 samples prepared at higher temperature feature smaller micropores, corresponding to stronger adsorption sites. The energetics of xenon adsorption can be independently evaluated from the evolution of the chemical shift of ^{129}Xe with temperature.

B. Variable-Temperature Experiments. Figure 5 shows the temperature-dependent spectra for 130 °C sample measured at a partial pressure of xenon of ca. 8 Torr. Increase of the temperature leads to the gradual high-field shift of the adsorbed line with the rate of ca. 0.3 ppm/deg and its broadening, whereas

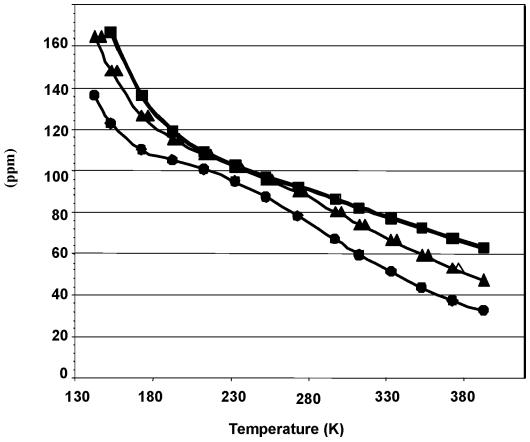

Figure 6. Temperature-dependent ^{129}Xe NMR chemical shifts of the resonance line of xenon adsorbed on SBA-15 silicas synthesized at different temperatures: (■) 60, (▲) 110, and (●) 130 °C.

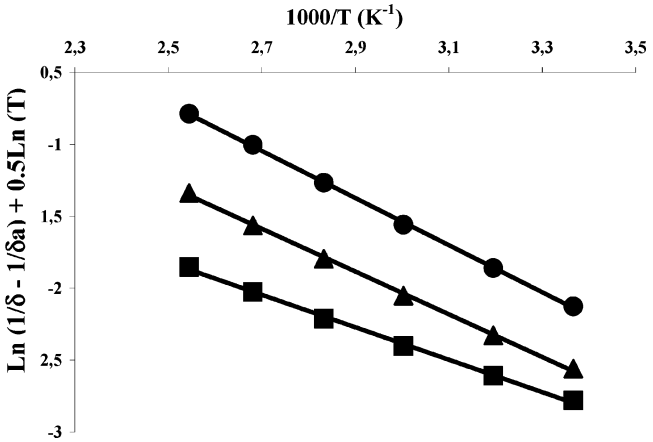

Figure 7. Determination of the heats of xenon adsorption (from eq 9) for SBA-15 silicas synthesized at different temperatures: (■) 60, (▲) 110 and (●) 130 °C.

the lowering of the temperature shifts the line to low field with a somewhat smaller rate to $T \sim 200$ K; after that temperature the rate significantly increases.

The line width of the adsorbed xenon at the temperature decrease first diminishes, and then starts to increase at temperatures around 200 K. The intensity of the signal significantly increases at low temperatures. The temperature-dependent spectra of the other two samples exhibit qualitatively similar behavior, as can be seen Figure 6. The evolution of the variable-temperature spectra reflects the changes of the adsorption constant with temperature which are obscured by the process of condensation of xenon at low temperatures, which occurs even at low partial pressures of xenon. This process is evidenced by the above-mentioned increase of the rate of evolution of the chemical shift at temperatures below 200 K, which originates from the increase of the xenon−xenon interactions in the adsorbed state. The proximity of the chemical shifts samples under study at temperatures around 230 K, when xenon spends most of the time in adsorbed state and does not "fill" the geometry of the environment, illustrates the fact that their surface properties are quite similar. Differences in the lower temperature region can be attributed to the peculiarities of the condensation process in the samples with different amounts of micropores: the latter should facilitate condensation of xenon. Indeed, the 60 and 110 °C samples exhibit higher values of the chemical shift at low temperatures than those of the 130 °C sample. The Henry constant K, which is temperature dependent, can be written as

$$K = K_0(T)^{-1/2} \exp(-\Delta H/RT) \qquad (9)$$

where K_0 is the preexponential factor which does not depend on the temperature. This temperature dependence allows one to obtain the effective heat of adsorption ΔH for the solids under consideration.

Equation 5 transforms to

$$\delta = \delta_a/[1 + D/(4K_0RT^{1/2}) \exp(-\Delta H/RT)] \qquad (10)$$

Linearization of this equation leads to

$$\ln(1/\delta - 1/\delta_a) + 0.5 \ln(T) = \Delta H/RT + \ln[D/(4\delta_a K_0 R)] \qquad (11)$$

In the high-temperature region, where the adsorption of xenon and, hence, xenon−xenon interactions in the adsorbed layer are low, these data can be used to obtain the heats of xenon adsorption. Figure 7 shows the determination of ΔH by plotting $\ln(1/\delta - 1/\delta_a) + 0.5 \ln T$ vs $10^3/T$ and by using the value $\delta_a = 125$ ppm from ref 10. The obtained ΔH values are presented in Table 2.

TABLE 2: Heats of Xenon Adsorption on SBA-15 Samples

sample temp (°C)	heat of adsorption (kJ/mol)
60	9.36
110	12.33
130	13.60

The measured values are in the same range as those obtained previously for other silica samples[10,11,18] and are typical for a process of physical adsorption. This allows excluding that the positive deviations of the chemical shift with pressure can be due to chemisorption phenomena, as in the case of metal-containing zeolites.

Conclusion

The evolution of the ^{129}Xe NMR chemical shift with pressure allows detection of the presence of unusually strong physisorption sites at the inner surface of mesopores. In the case of SBA-15, these adsorption sites can be identified with shallow micropores resulting from the interaction of silica with poly(oxyethylene) heads during the synthesis of the material. The slope of the dependence of the chemical shift from pressure provides information on the size of these micropores, at the borderline with the surface roughness. The decrease of the corrugation size with the increase of the temperature of synthesis provides new insight into the mechanism by which the microporosity of the precursors of SBA-15 collapses. The evolution of the chemical shift with the NMR measurement temperature allows evaluation of the heat of adsorption of xenon, which increases for SBA-15 synthesized at higher temperature, in parallel with the decrease of the size of the surface micropores. The use of hyperpolarized xenon is further confirmed as a powerful tool to obtain fast and reliable measurements in ^{129}Xe NMR spectroscopy.

References and Notes

(1) Impéror-Clerc, M.; Davidson, P.; Davidson, A. *J. Am. Chem. Soc.* **2000**, *122*, 11925.

(2) Kruk, M.; Jaroniec, M.; Ko, C. H.; Ryoo, R. *Chem. Mater*. **2000**, *12*, 1961.

(3) Ryoo, R.; Ko, C. H.; Kruk, M.; Antochshuck, V.; Jaroniec, M. *J. Phys. Chem. B* **2000**, *104*, 11465.

(4) Fenelov, V. B.; Derevyankin, A. Y.; Kirik, S. D.; Solovyov, L. A.; Shmakov, A. N.; Bonardet, J.-L.; Gédéon, A.; Romannikov, V. N. *Microporous Mesoporous Mater*. **2001**, *44*−*45*, 33.
(5) Ravikovitch, P. I.; Neimark, A. V. *J. Chem. Phys. B* **2001**, *105*, 6817.
(6) Galarneau, A.; Cambon, H.; Di Renzo, F.; Fajula, F. *Langmuir* **2001**, *17*, 8328.
(7) Galarneau, A.; Cambon, H.; Di Renzo, F.; Ryoo, R.; Choi, M.; Fajula, F. *New J. Chem.* **2003**, *27*, 73.
(8) Ito, T.; Fraissard, J. *Chem. Phys. Lett*. **1987**, *136*, 314.
(9) (a) Ripmeester, J.; Ratcliffe, C. *J. Phys. Chem.* **1990**, *94*, 7652. (b) Galarneau, A.; Cambon, H.; Martin, T.; De Menorval, L. C.; Brunel, D.; Di Renzo, F.; Fajula, F. *Stud. Surf. Sci. Catal*. **2002**, *141*, 395.
(10) Terskikh, V. V.; Mudrakovskii, I. L.; Mastikhin, V. M. *J. Chem. Soc., Faraday Trans*. **1993**, *89*, 4239.
(11) Cros, F.; Corb, J.-P.; Malier, L. *Langmuir* **2000**, *16*, 10193.
(12) Raftery, D.; MacNamara, E.; Fisher, G.; Rice, C. V.; Smith, J. *J. Am. Chem. Soc.* **1997**, *119*, 8746.
(13) Young, D. M.; Crowell, A. D. *Physical adsorption of gases*; Butterworths: Markham, ON, Canada, 1962; p 104.
(14) Langmuir. *J. Am. Chem. Soc*. **1918**, *40*, 1361.
(15) Springuel-Huet, M.-A.; Sun, K.; Fraissard, J. *Microporous Mesoporous Mater*. **1999**, *33*, 89.
(16) Conner, W. C.; Weist, E. I.; Ito, T.; Fraissard, J. *J. Phys. Chem.* **1998**, *93*, 4138.
(17) Israelachvili, J. N.; Wennerström, H. *J. Phys. Chem.* **1992**, *96*, 520.
(18) Nossov, A.; Haddad, E.; Guenneau, F.; Gedeon, A. *Phys. Chem. Chem. Phys.* **2003**, *5*, 4473−4478.